Inorganic Chemistry

pubs.acs.org/IC Article

Steric Effects of HN(CH₂CH₂PR₂)₂ on the Nuclearity of Copper Hydrides

Dewmi A. Ekanayake, Arundhoti Chakraborty, Jeanette A. Krause, and Hairong Guan*



Cite This: https://dx.doi.org/10.1021/acs.inorgchem.0c01865



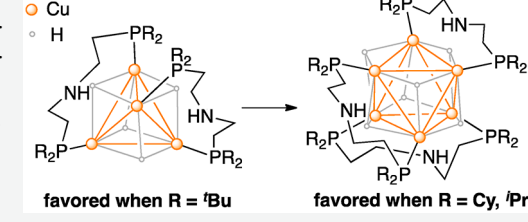
ACCESS

III Metrics & More

Article Recommendations

SI Supporting Information

ABSTRACT: Copper hydride clusters of the type $(^{R}PN^{H}P)_{n}Cu_{2n}H_{2n}$ $(^{R}PN^{H}P)_{n}Cu_{2n}H_{2n}$ $(^{R}PN^{H}P)_{n}Cu_{2n}H_{2n}$ $(^{R}PN^{H}P)_{n}Cu_{2n}H_{2n}$ $(^{R}PN^{H}P)_{n}Cu_{2n}H_{2n}$ $(^{R}PN^{H}P)_{n}Cu_{2n}H_{2n}$ $(^{R}PN^{H}P)_{n}Cu_{2n}H_{2n}$ $(^{R}PN^{H}P)_{n}Cu_{2n}H_{2n}$ with KO ^{t}Bu under H_{2} or in one pot from a 1:2:2 mixture of $^{R}PN^{H}P$, CuBr, and KO ^{t}Bu under H_{2} . With medium-sized phosphorus substituents $(^{R}=^{t}Pr$ and Cy), the phosphine ligands stabilize both hexanuclear and tetranuclear clusters; however, the smaller clusters are kinetic products and aggregate further over time. Use of a bulkier ligand $^{tBu}PN^{H}P$ leads to the formation of only a tetranuclear cluster. Crystallographic studies reveal a distorted octahedral Cu_{6} unit in $(^{tP}PN^{H}P)_{3}Cu_{6}H_{6}$ (2a) and $(^{Cy}PN^{H}P)_{3}Cu_{6}H_{6}$



(2b), while a tetrahedral Cu_4 unit exists in $(^{Cy}PN^HP)_2Cu_4H_4$ (2b') and $(^{tb}uPN^HP)_2Cu_4H_4$ (2c'), all furnished with face-capping hydrides and bridging $^RPN^HP$ ligands. The aggregations are maintained in solution, although hydrides are fluxional. These copper clusters are capable of reducing aldehydes and ketones to the corresponding copper alkoxide species. Ranking their reactivity toward N-methyl-2-pyrrolecarboxaldehyde gives 2b' > 2a, $2b \gg 2c'$, which correlates inversely with the order of thermal stability (against decomposition and cluster expansion).

■ INTRODUCTION

Copper hydrides have been proposed as key intermediates in numerous copper-catalyzed reactions that involve silanes, boranes, or dihydrogen. The empirical formula LCuH, which has been frequently used in the literature, is likely inadequate in defining the nature of the copper hydride species being generated during the catalytic processes. Well-defined copper hydride complexes are rarely monomeric. To date, the only successful strategy to prevent aggregation is through the use of an exceptionally bulky N-heterocyclic carbene (NHC) as the supporting ligand.² For phosphine-based systems, the best-known copper hydride, Stryker's reagent, is a hexanuclear copper cluster decorated by six hydrides and six triphenylphosphine ligands.³ Thus, it should be described using the chemical formula (Ph₃P)₆Cu₆H₆. A recent attempt to synthesize (dppbz)CuH (dppbz = 1,2-bis-(diphenylphosphino)benzene), a popular hydrosilylation catalyst, led to the isolation of (dppbz)₃Cu₃H₃. Schematic structures of (Ph₃P)₆Cu₆H₆ and (dppbz)₃Cu₃H₃ are shown in Figure 1 along with other neutral, phosphine-stabilized copper hydride clusters that have been crystallographically characterized. These structures are remarkably diverse, featuring Cu_2H_2 (**A**⁶ and **B**⁷), Cu_3H_3 (**C**), 5 Cu_5H_5 (**D**), 8 Cu_6H_6 (**E**), 3,5 , and Cu_8H_8 (F)^{9c} cores. There is ample evidence suggesting that the aggregation is maintained in solution, although dissociation to the monomeric form is conceivable. The correlation between the size of the cluster and the property of the phosphine ligand is, however, not well understood.

In the materials chemistry field, many copper-based nanoscale frameworks with face-capping and/or interstitial hydrides have been developed for applications in hydrogen storage and catalysis. These expanded copper hydride clusters (Cu_{20} – Cu_{32}) are often stabilized by sulfur- or selenium-based ligands. It is also possible to utilize two different ligands or a combination of hard and soft donors to construct a relatively large copper hydride cluster. A recent study by Hayton and co-workers showed that the reaction of $(Ph_3P)_6Cu_6H_6$ with 1,10-phenanthroline (phen) in CH_2Cl_2 produced $[Cu_{14}H_{12}(phen)_6(PPh_3)_4][Cl]_2$. The structures of these copper hydride clusters or nanoclusters are interesting in their own right, although establishing the relationship between the size of the copper hydride core and ligand property remains a challenge.

One of our ongoing research projects is to develop catalytic hydrogenation reactions with base metals supported by PNP-type pincer ligands $HN(CH_2CH_2PR_2)_2$ (or $^RPN^HP$ for short). The interest in this specific type of ligands is driven by the notion that the nitrogen site can participate in dihydrogen activation as well as proton transfer. In studying the copper system, we have encountered two different copper

Received: June 23, 2020



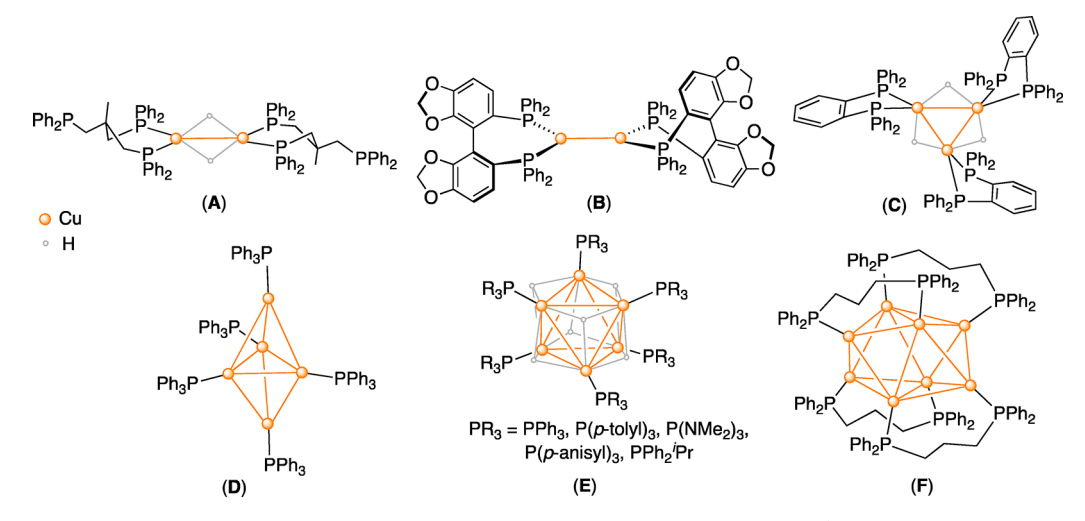


Figure 1. Crystallographically characterized neutral copper hydride clusters bearing phosphine ligands (hydrides in B, D, and F were not refined).

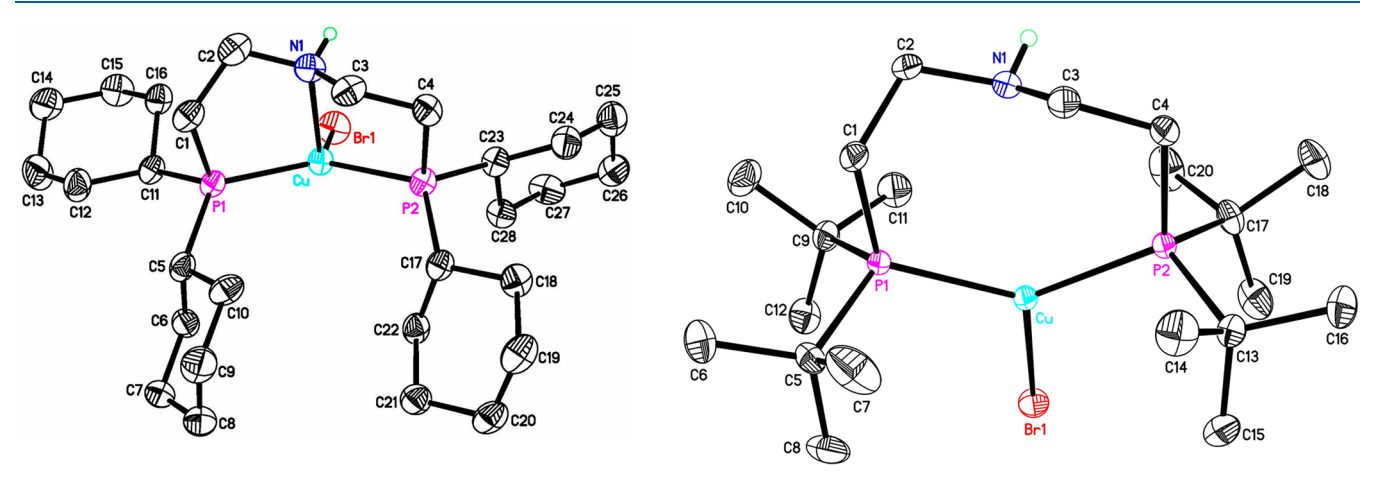


Figure 2. ORTEP drawings of $(^{Cy}PN^{H}P)$ CuBr (1b, left) and $(^{Bu}PN^{H}P)$ CuBr (1c, right) at the 50% probability level (all hydrogen atoms except the one bound to nitrogen omitted for clarity).

hydride clusters stabilized by the same ligand. Previous work by others suggest that $(Ph_3P)_5Cu_5H_5$ and $(Ph_3P)_6Cu_6H_6$ coexist from the reaction of $(Ph_3P)_3CuCl$ with K-selectride, although it is unclear if these two clusters can interconvert. Our work presented herein provides a unique platform to probe the interconversion of different copper hydride clusters during hydride formation and hydride transfer. Through variation of the phosphorus substituents in $^RPN^HP$ (R = iPr , Cy, and tBu), we are beginning to understand how the steric effects influence the nuclearity of the copper hydrides.

RESULTS AND DISCUSSION

Synthesis of Copper Hydride Complexes. In the 1980s, Caulton and co-workers pioneered a strategy to prepare copper hydrides through hydrogenolysis of $(CuO^tBu)_4$ in the presence of a phosphine ligand. Later, Stryker et al. developed a convenient method to make $(Ph_3P)_6Cu_6H_6$, which involved the mixing of CuCl with PPh₃ followed by the addition of NaO^tBu and dihydrogen. The first step presumably produced a triphenylphosphine-ligated copper chloride complex. For the RPNHP ligand system, molecules of this type became our initial targets. The Arnold group already reported the synthesis of $(^{iP}PN^HP)CuBr$ (1a) via direct complexation of $^{iP}PN^HP$ to CuBr. This compound was also made in our laboratory, and following a similar procedure, $(^{Cy}PN^HP)CuBr$ (1b) and

(fBuPNHP)CuBr (1c) were isolated as white solids in good yields (eq 1).

$$\begin{array}{c} H \\ PR_2 \\ N \end{array} \xrightarrow{PR_2} \begin{array}{c} CuBr \\ THF, RT \\ 16 \text{ h} \end{array} \xrightarrow{R_2P} \begin{array}{c} H \\ N \\ R_2P \end{array} \xrightarrow{P} \begin{array}{c} H \\ N \\ Cu - Br \end{array} \xrightarrow{P} \begin{array}{c} PR_2 \\ P \\ PBu_2 \end{array}$$

$$R = Pr (1a)$$

$$R = Cy (1b)$$

$$1c$$

Crystallographic studies of 1a-c show that the structures of these copper bromide complexes vary with the phosphorus substituents. As illustrated in Figure 2 (left), 1b features a fourcoordinate Cu(I) center. On the basis of the geometry index $(\tau_4 = 0.80)$ proposed by Houser, ¹⁸ the coordination geometry is best described as trigonal pyramidal. The previously reported structure of 1a exhibits a very similar geometry with τ_4 values of 0.82 and 0.81 calculated for the two independent molecules (Table 1).¹⁷ The NH hydrogen in 1a and 1b adopts a syn configuration with respect to the bromide, although it is hydrogen-bonded to the bromide from a neighboring molecule. The Cu-N bond distance is slightly shorter in 1a, likely due to less steric congestion imposed by the isopropyl groups. In contrast, with a bulkier phosphorus substituent, 1c displays a trigonal planar geometry devoid of a nitrogencopper interaction (Figure 2, right), as evidenced by a long interatomic distance of 3.2212(15) Å. This is also reflected by

Table 1. Selected Bond (Or Contact) Lengths (Å) and Angles (deg) of 1a-c

	1a ^a	1b	1c
Cu···N1	2.274(2), 2.256(2)	2.290(5)	3.2212(15)
Cu-Br1	2.4432(4), 2.4488(4)	2.4164(9)	2.4196(3)
Cu-P1	2.2448(6), 2.2461(6)	2.2248(16)	2.2617(4)
Cu-P2	2.2470(6), 2.2532(5)	2.2416(15)	2.2583(4)
P1-Cu-P2	125.39(2), 126.13(2)	132.05(6)	133.629(17)
P1-Cu-Br1	118.36(2), 119.71(2)	115.10(5)	112.365(13)
P2-Cu-Br1	115.77(2), 113.74(2)	112.00(5)	113.942(13)
\sum_{P2CuBr}^{b}	359.52, 359.58	359.15	359.94
N1···Cu-Br1	105.68(4), 104.79(4)	113.26(12)	150.95(3)
N1···Cu-P1	86.18(4), 86.14(4)	83.94(13)	68.40(3)
N1···Cu-P2	86.12(4), 86.74(4)	85.74(12)	70.18(3)

"Data taken from ref 17; two sets of data provided here due to the presence of two independent molecules in the crystal lattice. ^bSum of the angles P1–Cu–P2, P1–Cu–Br1, and P2–Cu–Br1.

a far more obtuse N···Cu-Br angle and more acute N···Cu-Pr angles (Table 1). Structure 1c also shows an intermolecular hydrogen-bonding interaction between the NH group and the bromide.

Spectroscopic data suggest that in solution 1c also behaves differently from the isopropyl and cyclohexyl derivatives. The phosphorus resonances of ^{iPr}PN^HP (-1.1 ppm, in C₆D₆) and $^{C_y}PN^HP$ (-9.5 ppm, in C_6D_6) shift downfield upon coordination to copper (1a: 4.3 ppm; 1b: -4.1 ppm). The opposite trend was observed for the tert-butyl case (tBuPNHP: 22.7 ppm; 1c: 15.0 ppm). These chemical shift changes are known to be sensitive to the chelating ring size. 19 A fivemembered ring created by complexation usually causes a downfield shift of the phosphorus resonance. However, not enough data are available for eight-membered chelate ring systems like the one shown by the solid-state structure of 1c (Figure 2). A closely related example is xantphos or 4,5bis(diphenylphosphino)-9,9-dimethylxanthene, which appears at -16.8 ppm (in CDCl₃)²⁰ as the free ligand and shifts upfield by 1 ppm upon conversion to (xantphos)CuBr·2MeCN.²¹ Other anomalies of 1c include a singlet observed for the PCH₂ carbon resonance instead of a triplet for the corresponding resonance in 1a and 1b. Furthermore, IR spectroscopy implies that the NH bond in 1c (3271 cm⁻¹) is stronger than that in 1a (3227 cm⁻¹) or 1b (3221 cm⁻¹), and indicative of an uncoordinated secondary amine. ²² Taken together, these results are consistent with a κ^{P} , κ^{P} -coordination mode for the ^{tBu}PN^HP ligand in 1c.

Having prepared and characterized the copper bromide complexes, we shifted our attention to the formation of copper hydrides by mixing $1\mathbf{a}-\mathbf{c}$ with KO^tBu under a hydrogen atmosphere (Scheme 1). The reaction of $1\mathbf{a}$, which was kept under 40 psig of H_2 for 1 h, produced a bright orange solution. The ³¹P{¹H} NMR spectrum of isolated product $2\mathbf{a}$ displayed a singlet at 1.0 ppm (in C_6D_6) with the typical broadening caused by the quadrupolar ⁶³Cu and ⁶⁵Cu nuclei. The ¹H NMR spectrum supported a ($^{1\text{PP}}N^{\text{HP}}$) $_3Cu_6H_6$ formulation based on a septet at 2.07 ppm ($J_{P-H}=7.0$ Hz) assigned to the hydride and a 2:1 hydride-to- $^{1\text{PP}}N^{\text{HP}}$ P ratio. The hydride resonance was confirmed by comparing the spectra of ($^{1\text{PP}}N^{\text{HP}}$) $_3Cu_6H_6$ and ($^{1\text{PP}}N^{\text{HP}}$) $_3Cu_6D_6$ (prepared from $1\mathbf{a}$, KO^tBu, and D_2) and recording the ²H NMR spectrum of ($^{1\text{PP}}N^{\text{HP}}$) $_3Cu_6D_6$. Attempts to locate the Cu–H bands by IR spectroscopy were unsuccessful, likely due to weak intensity.

Scheme 1. Synthesis of Copper Hydride Clusters from (RPNHP)CuBr

$$(^{\text{Pr}PNHP})\text{CuBr} \xrightarrow{H_2 \text{ (40 psig)}} \text{toluene, RT} \xrightarrow{\textbf{1 h}} (^{\text{Pr}PNHP})_3\text{Cu}_6\text{H}_6 \\ \textbf{1a} & \text{1 h} & \textbf{2a} \\ (^{\text{Bu}PNHP})\text{CuBr} \xrightarrow{\textbf{H}_2 \text{ (80 psig)}} \text{toluene, RT} \xrightarrow{\textbf{2c'}} (^{\text{Bu}PNHP})_2\text{Cu}_4\text{H}_4 \\ \textbf{1c} & \text{4 h} & \textbf{2c'} \\ & \text{KO'Bu} \\ (^{\text{CyPNHP}})\text{CuBr} \xrightarrow{\textbf{H}_2 \text{ (40 psig)}} \text{toluene, RT} \xrightarrow{\textbf{1 h}} (^{\text{CyPNHP}})_3\text{Cu}_6\text{H}_6 + (^{\text{CyPNHP}})_2\text{Cu}_4\text{H}_4 \\ \textbf{1b} & \text{1 h} & \textbf{2b} & \textbf{2b'}$$

tert-Butyl derivative 1c required a higher H_2 pressure and a longer time to react (Scheme 1), resulting in a mustard yellow solution. Isolated product 2c' was an off-white solid which when dissolved in C_6D_6 showed a hydride resonance at 4.94 ppm as a quintet ($J_{P-H}=14.4~Hz$). The NH resonance appeared as a separate quintet at 3.54 ppm with a vicinal coupling constant of 8.4 Hz. Mixing 2c' with D_2O resulted in a rapid H/D exchange with the NH hydrogen but not with the hydride, although after an extended period of time (24 h), decomposition of 2c' to the free ligand was observed. Most importantly, the hydride and the $^{tBu}PN^HP$ ligand were integrated to a 2:1 ratio, implying that the formula for 2c' is $(^{tBu}PN^HP)_2Cu_4H_4$.

Under 40 psig of H₂, the reaction of **1b** with KO^tBu yielded a bright orange-red solution. Adding acetonitrile to induce precipitation of the product, as used for the purification of 2a and 2c', generated a pink precipitate along with an orange-red oily material. The presence of two different morphologies hinted that the cyclohexyl analog formed multiple copper hydride clusters in appreciable amounts, likely including $(^{Cy}PN^{H}P)_{3}Cu_{6}H_{6}$ (2b) and $(^{Cy}PN^{H}P)_{2}Cu_{4}H_{4}$ (2b'). In pentane, the tetranuclear species has a lower solubility than the hexanuclear species, which allowed us to enrich 2b' to an analytically pure form as a white solid (for details, see the Experimental Section). Despite repeated efforts, we have not yet been able to obtain pure 2b; the isolated product was always contaminated with 2b' (20-40 mol %) and consequently exhibited various shades of red in color (see the Supporting Information). The characteristic hydride resonances (in C₆D₆) were located at 5.04 ppm (quintet, $J_{P-H} = 14.4 \text{ Hz}$) for **2b**' and at 2.06 ppm (septet, $J_{P-H} = 7.2$

Balancing the equations in Scheme 1 would suggest that half of the RPNHP ligands dissociated from copper during hydride formation. Indeed, free phosphine ligands were detected when these reactions were monitored by NMR spectroscopy. To make the best use of the RPNHP ligands, an alternative, one-pot method was developed by mixing RPNHP, CuBr, and KO'Bu in a 1:2:2 ratio followed by the addition of H₂:

$${}^{R}PN^{H}P + \underset{(1:2:2)}{\text{CuBr}} + KO^{t}Bu \xrightarrow{H_{2} (40-80 \text{ psig})} \xrightarrow{\text{toluene, RT}} \frac{1}{n} ({}^{R}PN^{H}P)_{n} Cu_{2n} H_{2n}$$

$${}^{H}PN^{H}P + \underset{(n=2 \text{ or } 3)}{\text{Cu}_{2n}} H_{2n}$$

The conditions were similar to those outlined in Scheme 1, except that the reaction time should be kept within 1 h. This is critical to the synthesis of 2c' because significant decomposition was noticed after 90 min.

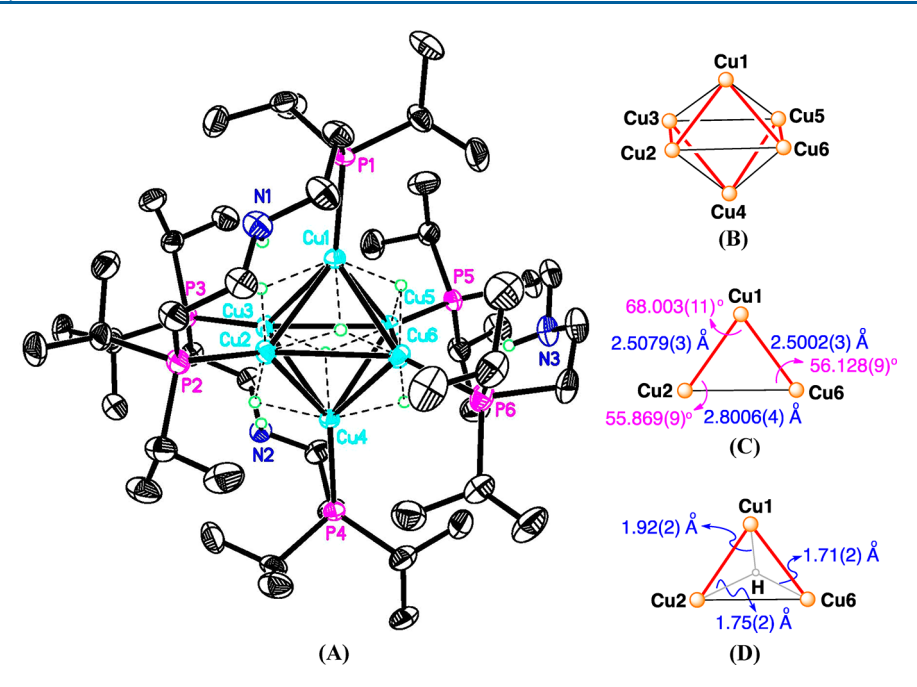


Figure 3. (A) ORTEP drawing $(^{PP}PN^{H}P)_{3}Cu_{6}H_{6}\cdot C_{7}H_{8}$ (2a· $C_{7}H_{8}$) at the 50% probability level (cocrystallized toluene molecule and all hydrogen atoms except those on nitrogen and copper omitted for clarity), (B) the Cu_{6} unit with the short Cu-Cu contacts highlighted in red, (C) structural parameters for a representative hydride-capped Cu_{3} face, and (D) Cu-H bond distances in a representative $Cu_{3}(\mu_{3}-H)$ unit.

Table 2. Selected Bond (Or Contact) Lengths (Å) and Angles (deg) of the Copper Hydride Clusters

	•	. & . ,	2 . 0,	/		
		2a·C ₇ H ₈		2b	2b'	2c′
Cu-P	2.2437(6)		2.2433(6)		2.1790(4)	2.1995(4)
	2.2514(5)		2.2455(5)		2.1800(4)	2.2015(5)
	2.2599(5)		2.2661(5)		2.1892(4)	2.2060(4)
	2.2605(5)		2.2681(6)		2.1897(4)	2.2071(5)
	2.2717(5)		2.2723(6)			
	2.2734(5)		2.2806(5)			
	2.5002(3)	2.7393(4)	2.4927(3)	2.7361(3)	2.4542(3)	2.4710(3
	2.5052(4)	2.7545(3)	2.4979(3)	2.8041(3)	2.4637(3)	2.4863(3
Cu-Cu ^a	2.5079(3)	2.7735(3)	2.5004(3)	2.8073(3)	2.4689(3)	2.4864(3
	2.5094(3)	2.8006(4)	2.5261(3)	2.8088(3)	2.4815(3)	2.4894(3
	2.5170(4)	2.8223(3)	2.5312(3)	2.8112(3)	2.4835(3)	2.4898(3
	2.5282(3)	2.8333(3)	2.5337(3)	2.8112(4)	2.5072(3)	2.4980(3
	55.526(9)	66.223(10)	55.566(9)	65.993(10)	58.908(8)	59.438(8
	55.797(9)	66.775(10)	55.606(9)	67.233(10)	59.348(7)	59.550(8
	55.830(9)	66.809(10)	55.628(9)	67.439(10)	59.438(8)	59.802(8
	55.869(9)	68.003(11)	55.802(9)	67.823(10)	59.501(7)	59.913(8
	56.128(9)	68.027(10)	55.866(9)	68.528(10)	59.553(8)	59.935(8
	56.176(9)	68.644(10)	56.153(9)	68.569(10)	60.027(8)	60.036(8
	56.270(9)	88.627(10)	56.342(9)	88.686(10)	60.063(7)	60.045(8
	56.527(9)	89.132(10)	56.408(9)	88.749(10)	60.209(8)	60.052(8
C C Ca,b	56.698(9)	89.230(10)	56.425(9)	88.820(10)	60.291(7)	60.166(8
Cu-Cu-Cu ^{a,b}	56.815(9)	89.277(10)	56.507(9)	89.426(10)	60.535(8)	60.263(8
	56.920(9)	89.632(10)	56.611(9)	89.541(10)	61.028(8)	60.284(8
	56.963(9)	89.707(10)	57.500(9)	89.680(10)	61.100(8)	60.516(8
	58.308(9)	90.082(10)	58.322(8)	90.458(10)		
	58.837(8)	90.495(10)	59.937(8)	90.497(10)		
	59.498(9)	90.709(10)	59.990(9)	90.711(10)		
	60.451(9)	90.796(10)	60.074(9)	91.080(10)		
	61.241(9)	90.797(11)	60.709(9)	91.134(11)		
	61.664(9)	91.344(11)	60.968(9)	91.152(10)		

^aNumbers in bold font are for uncapped Cu₃ faces. ^bNumbers in italic font are for Cu–Cu–Cu angles in a square formed by four copper atoms.

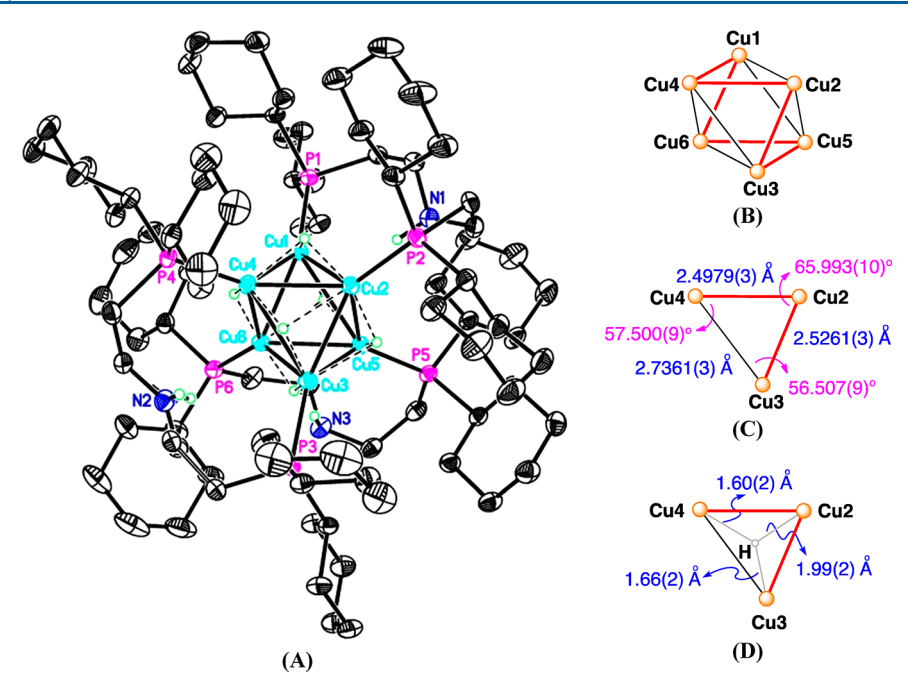


Figure 4. (A) ORTEP drawing $(^{\text{Cy}}\text{PN}^{\text{H}}\text{P})_3\text{Cu}_6\text{H}_6$ (2b) at the 50% probability level (all hydrogen atoms except those on nitrogen and copper omitted for clarity; N2 and one of the neighboring carbons are disordered). (B) Cu₆ unit with the short Cu–Cu contacts highlighted in red. (C) Structural parameters for a representative hydride-capped Cu₃ face. (D) Cu–H bond distances in a representative Cu₃(μ_3 -H) unit.

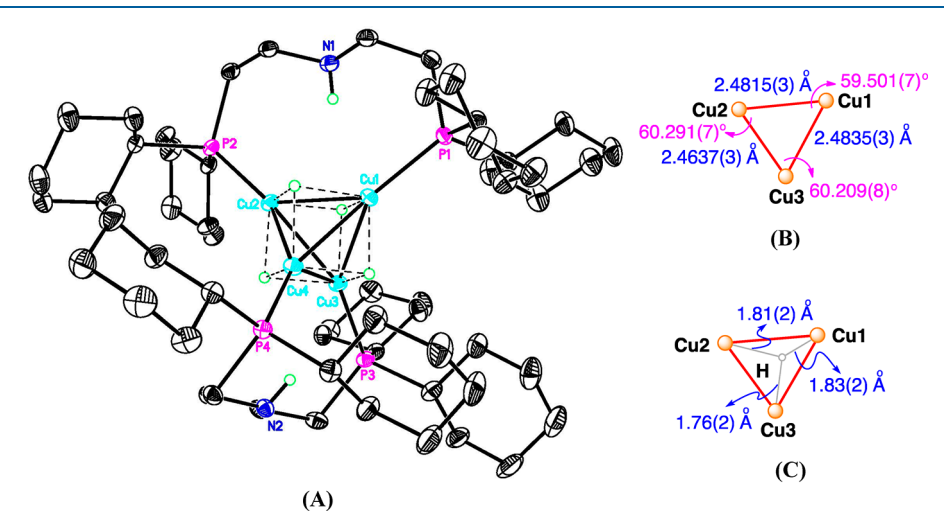


Figure 5. (A) ORTEP drawing $(^{Cy}PN^{H}P)_{2}Cu_{4}H_{4}$ (2b') at the 50% probability level (all hydrogen atoms except those on nitrogen and copper omitted for clarity), (B) structural parameters for a representative Cu_{3} face, and (C) Cu-H bond distances in a representative $Cu_{3}(\mu_{3}-H)$ unit.

Structures of the Copper Hydride Clusters. The solid-state structures of 2a, 2b, 2b', and 2c' were studied by X-ray crystallography. As illustrated in Figure 3A, the centerpiece of 2a is a distorted octahedron constructed of six copper atoms. Hydride ligands were located directly from the difference map and found to cap six of the eight faces, leaving two antiparallel Cu₃ faces unoccupied (i.e., Cu1–Cu3–Cu5 and Cu2–Cu4–Cu6). The coordination spheres are completed by three iPPNHP ligands, each bridging two contiguous copper centers. Overall, this structure is reminiscent of Stryker's reagent, which bears a similar octahedral Cu₆ unit with six face-capping hydrides.⁸

Structure of $(Ph_3P)_6Cu_6H_6\cdot DMF$ reported by Churchill et al. showed six short Cu-Cu contacts (2.494(6)-2.595(5) Å) and six long Cu-Cu contacts $(2.632(6)-2.674(5) \text{ Å}).^{3b}$ A later study by Healy, White, and co-workers demonstrated that

the cocrystallized solvent molecule (THF instead of DMF) could distort the octahedral unit further to have six shorter Cu–Cu contacts (2.477(2)-2.495(2) Å) and six longer Cu–Cu contacts (2.707(2)-2.783(2) Å). These data, along with those reported for other $(R_3P)_6\text{Cu}_6\text{H}_6$, lead to a generalized conclusion that the long Cu–Cu contacts form the Cu₃ faces without a capping hydride. This phenomenon certainly extends to 2a (Figure 3B), which also has six short Cu–Cu contacts (2.5002(3)-2.5282(3) Å), see Table 2) as well as six long Cu–Cu contacts (2.7393(4)-2.8333(3) Å) forming the two uncapped Cu₃ faces. It should be noted here that some of these copper—copper separations are close to twice the van der Waals radius for copper $(1.4 \text{ Å})_5^{24}$ hence, weak Cu–Cu interactions exist, if any.

As expected, the two uncapped Cu_3 faces are close to equilateral triangles with Cu-Cu-Cu angles falling in the

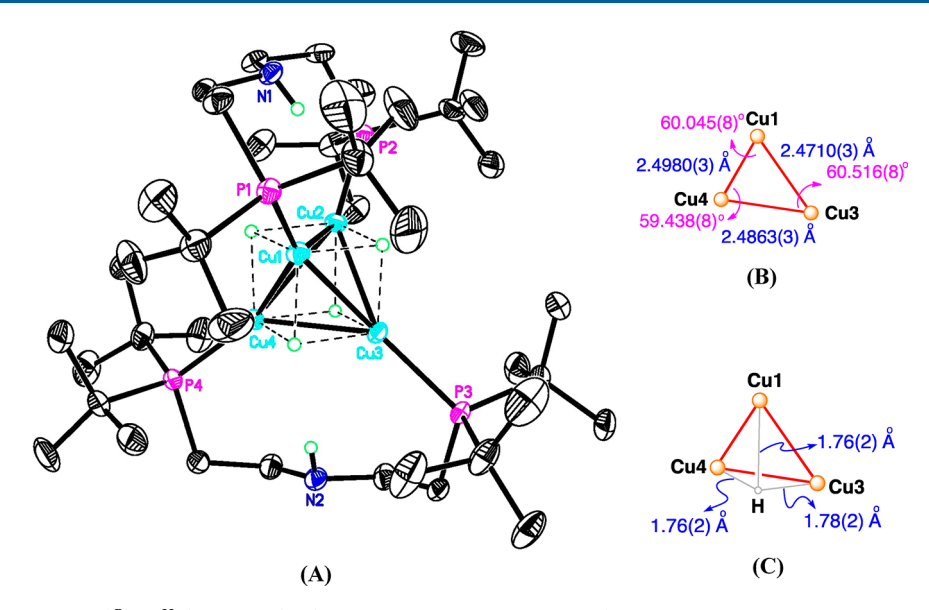


Figure 6. (A) ORTEP drawing $(^{tBu}PN^HP)_2Cu_4H_4$ (2c') at the 50% probability level (all hydrogen atoms except those on nitrogen and copper omitted for clarity), (B) structural parameters for a representative Cu_3 face, and (C) Cu-H bond distances in a representative $Cu_3(\mu_3-H)$ unit.

range of 58.308(9)–61.664(9)° (Table 2). In contrast, the hydride-capped Cu₃ faces are isosceles triangles constructed by two short Cu–Cu contacts and one long Cu–Cu contact (Figure 3C). The exact locations of the hydrides in this type of clusters have been subject for debate in the literature. On the basis of a neutron diffraction study of [(p-tolyl)₃P]₆Cu₆H₆, Bau and co-workers proposed a face-capping mode for the hydrides. A revisit of the (Ph₃P)₆Cu₆H₆ structure by the Parker group included techniques like inelastic neutron scattering, infrared spectroscopy, and *ab initio* calculations, which collectively supported an edge-bridging mode for the hydrides. X-ray diffraction does not provide the precision needed to pinpoint the coordination mode for the hydrides. Nevertheless, our data show two short Cu–H bonds and one long Cu–H bond on a Cu₃ face (Figure 3D).

Unlike 2a, hexanuclear cluster 2b crystallized without solvent in the lattice (Figure 4). The slightly increased steric bulk (changing from isopropyl to cyclohexyl groups) appears to have almost no impact on the key structural parameters (Table 2). The Cu₆ unit (Figure 4B) also features six short Cu-Cu contacts (2.4927(3)-2.5337(3) Å) and six long Cu-Cu contacts (2.7361(3)-2.8112(4) Å). The three copper atoms in any of the hydride-capped Cu₃ faces form an isosceles triangle, as exemplified by Figure 4C, while the hydride ligand is bound asymmetrically with two short Cu-H bonds and one long Cu–H bond (Figure 4D). Interestingly, the three ^{Cy}PN^HP ligands bridge contiguous copper centers that form one short Cu-Cu contact and two long Cu-Cu contacts. This stands in contrast to 2a where the two copper centers bridged by each ^{iPr}PN^HP ligand form a short Cu-Cu contact only. In any case, these PNP-type ligands appear to have a backbone flexible enough to accommodate variable copper-copper distances.

In the presence of $^{\text{Cy}}\text{PN}^{\text{H}}\text{P}$ ligand, copper hydride forms a second cluster, 2b', bearing a tetrahedral Cu_4 unit with triply bridging hydrides or a cubic Cu_4H_4 core with copper atoms and hydrides occupying the alternate corners (Figure 5A). Several tetranuclear copper hydride complexes have been reported in the literature, including $[\text{Cu}_4\text{HX}_2(\text{Ph}_2\text{PPy})_4]^+$ (X = Cl, Br), 27 $[\text{Cu}_4\text{H}_3(\text{dpmp})_3]^+$ (dpmp = PhP(CH₂PPh₂)₂), 28 $[\text{Cu}_4\text{H}_3(\text{dpmppm})_2]^+$ (dpmppm = Ph₂PCH₂(Ph)PCH₂P(Ph)-

 $(CH_2PPh_2)^{29}$ $[Cu_4H_2(dpmppe)_2]^{2+}$ (dpmppe = $(CH_2PPhCH_2PPh_2)_2)_3^{30}$ $[Cu_4H_2(dpmppe)_2(RNC)_2]^{2+}$ $(R = {}^tBu, Cy)_3^{0}$ and $Cu_4H_2({}^{tBu}PNNP^*)_2$ $({}^{tBu}PNNP^*)_3$ is an anionic, naphthyridine-linked diphosphine). These systems share the commonality of having a cationic Cu_4H_x (x = 1-3) core with significant deviation of the Cu₄ unit from the ideal tetrahedral geometry. In particular, the four copper atoms in $[Cu_4H_3(dpmppm)_2]^{+,29}$ $[Cu_4H_2(dpmppe)_2L_2]^{2+}$ (L = none or RNC),³⁰ and Cu_4H_2 (^{fBu}PNNP*)₂³¹ are arranged to form a rectangle, rhombus, and butterfly shape, respectively. A neutral Cu₄H₄ core with such high degree of symmetry as that shown in 2b' is unprecedented. Essentially, every three copper atoms form an equilateral triangle (Figure 5B), and the overall symmetric Cu₄ unit is reflected by a relatively narrow range of Cu-Cu contacts (2.4542(3)-2.5072(3) Å) and Cu-Cu-Cu angles $(58.908(8)-61.100(8)^{\circ})$. In addition, the hydride ligands are more centrally located on the Cu₃ faces (Figure 5C). The Cu-P bonds in 2b' (2.1790(4)-2.1897(4) Å) are substantially shorter than those in **2b** (2.2433(6)-2.2806(5))Å), possibly due to reduced steric clash between the CyPNHP ligands.

The use of $^{tBu}PN^{H}P$ as the supporting ligand resulted in an analogous copper hydride cluster 2c' (Figure 6). The highly symmetric Cu_4H_4 core is manifested in an even narrower range of Cu-Cu contacts (2.4710(3)-2.4980(3) Å) and Cu-Cu-Cu angles $(59.438(8)-60.516(8)^{\circ})$. The Cu-P bonds seem unaffected by the phosphorus substituents as they are only marginally longer than those in 2b' (Table 2).

It is of interest that for the copper hydride clusters described above the NH groups are pointing toward the Cu_6H_6 or Cu_4H_4 core. As a representative example, in Figure 7, one of the NH hydrogens in 2b' is shown to have a close contact with the nearby hydride, possibly due to a dihydrogen bonding interaction. At this point, it is unclear to us if such an interaction plays any role in stabilizing the clusters. We plan to address this by replacing the NH group with a CH_2 group, and these results will be reported in due course.

Previous NMR studies of $(R_3P)_6Cu_6H_6$ and related compounds suggest that the hexanuclear structure is preserved in solution and the rapid intramolecular hydride migration

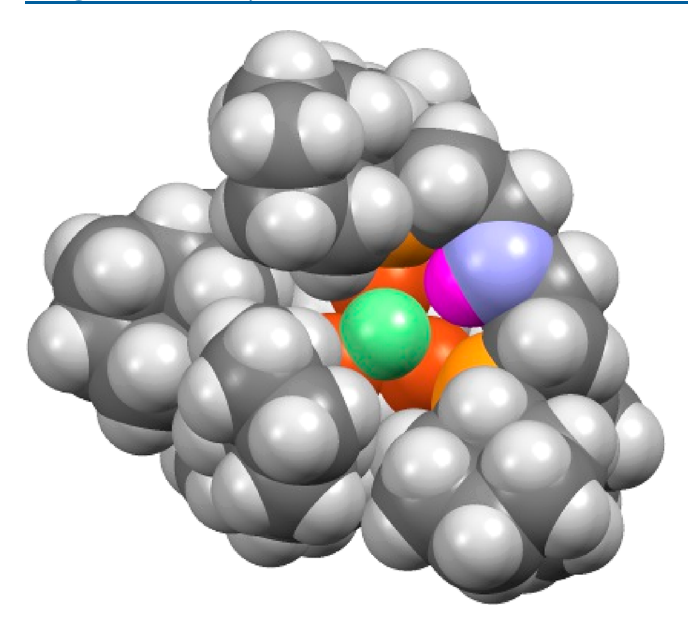
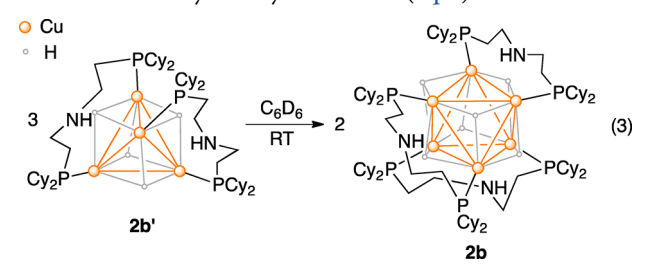


Figure 7. Space-filling model of 2b' (hydride, light green; NH hydrogen, magenta).

renders the six phosphorus nuclei equivalent. S,15,33 Presumably, for the $^{R}PN^{H}P$ -based system presented here, the crystal structures also reflect how the copper hydrides aggregate in solution. Taking the fluxional behavior of the hydrides into consideration, the nuclearity revealed by the crystallographic study is in agreement with our solution NMR data, which show hydride resonances as a septet for 2a/2b and a quintet for 2b'/2c'.

Tetranuclear-to-Hexanuclear Conversion. Copper hydrides stabilized by NHC ligands often bear a Cu_2H_2 core. The Bertrand group showed that increasing the steric bulk of the NHC ligands led to an equilibrium mixture of dinuclear and mononuclear species, although the latter is not amenable to isolation. For phosphine-based systems, Healy, White, and co-workers obtained both $(Ph_3P)_5Cu_5H_5$ and $(Ph_3P)_6Cu_6H_6$ from the reaction of $(Ph_3P)_3CuCl$ with K-selectride. It is not yet known if the pentamer can be converted to the hexamer or vice versa. In this study, we directly observed the conversion of $(^RPN^HP)_2Cu_4H_4$ to $(^RPN^HP)_3Cu_6H_6$, a process highly sensitive to the phosphorus substituents.

The tetranuclear-to-hexanuclear conversion was most evident with the cyclohexyl derivative (eq 3):



Cluster $2\mathbf{b}'$, when freshly purified, was almost colorless in toluene (or C_6D_6) solution, but turned pink if left at room temperature for 20 min or at -30 °C for 24 h. Monitoring the room temperature reaction by NMR spectroscopy (see the Supporting Information) showed that in 12 h ~20% of $2\mathbf{b}'$ was converted to $2\mathbf{b}$ along with a small amount of the free ligand $^{\text{CyPNHP}}$. Efforts to gain mechanistic insights by studying the kinetics of the cluster expansion were hampered by significant decomposition of the hydrides to Cu(0), H₂, and $^{\text{CyPNHP}}$, even in the presence of H₂. Both $2\mathbf{b}'$ and $2\mathbf{b}$ in their solid form were found to be stable at -30 °C for months but decomposed to a brown material if left at room temperature for a few days.

With a bulkier phosphine ligand, tetranuclear cluster 2c' showed a much higher thermal stability. The solution of 2c' in C_6D_6 kept at room temperature under ambient light conditions did not change color after 24 h. However, irradiation of the sample with 365 nm UV LEDs for 12 h led to the darkening of the solution and the observation of H_2 and ${}^{tBu}PN^HP$ by NMR.

$$\begin{array}{c} \text{H} \\ \text{Pr}_{12}\text{P} \\ \text{Pr}_{2}\text{P} \\ \text{Pr}_{2}\text{P} \\ \text{Pr}_{2}\text{P} \\ \text{1a} \end{array} + \begin{array}{c} \text{KO'Bu} + \text{H}_{2} & \frac{\text{C}_{6}\text{D}_{6}, \text{RT}}{\text{G}_{3}\text{O min}} \\ \text{Moreover} \\ \text{Pr}_{2}\text{P} \\ \text{1a} \end{array} + \begin{array}{c} \text{(PrPNHP)}_{2}\text{Cu}_{4}\text{H}_{4} + \text{(PrPNHP)}_{3}\text{Cu}_{6}\text{H}_{6}} \\ \text{2a} \\ \text{2a} \\ \text{+ KBr + 'BuOH + 'PrPNHP} \\ \text{1a} \end{array}$$

There was no evidence suggesting that the hexanuclear cluster $(^{tBu}PN^{H}P)_{3}Cu_{6}H_{6}$ (2c) formed.

If the tetranuclear-to-hexanuclear conversion or cluster expansion were favored by a less sterically hindered phosphine ligand, then one would predict that it should also occur to the isopropyl derivative. We never succeeded in isolating (iPrPNHP)2Cu4H4 (2a'), possibly because its conversion to 2a outpaced our workup of the reaction. To observe 2a' spectroscopically, 1a was treated with KO^tBu in C_6D_6 and then exposed to H₂ (eq 4). The spectra recorded after 30 min showed 2a' (14% of total phosphorus) in addition to 2a (25% of total phosphorus) and ^{fPr}PN^HP. Similar to 2b' and 2c', 2a' displayed a hydride resonance at 5.11 ppm as a quintet $(J_{P-H} =$ 14.2 Hz). Its phosphorus resonance was located at 10.8 ppm, which is shifted downfield from the free ligand by 11.9 ppm. The trend of phosphorus resonances (going from iPrPNHP to (iPrPNHP)3Cu6H6 and to (iPrPNHP)2Cu4H4) is very similar to what was observed with the cyclohexyl case (Table 3). Cluster 2a' eventually disappeared from the reaction mixture, leaving 2a and ^{iPr}PN^HP as the main phosphorus-containing species. The hexanuclear cluster 2a was also found to be thermally unstable, especially in the absence of H₂. In fact, to avoid significant decomposition, the ¹³C{¹H} NMR spectrum is best recorded at 10 °C.

Reactions with Carbonyl Compounds. One of the catalytic applications with copper hydrides is the hydrogenation or hydrosilylation of carbonyl compounds. The commonly proposed mechanism involves C=O insertion into

Table 3. Key NMR Resonances of the Free Ligands and the Copper Hydride Clusters (in C₆D₆)

	$R = {}^{i}Pr$		R = Cy		$R = {}^{t}Bu$	
	$\delta_{ m p}$	$\delta_{ m hydride}$	$\delta_{ ext{p}}$	$\delta_{ m hydride}$	$\delta_{ m p}$	$\delta_{ m hydride}$
$^{R}PN^{H}P$	-1.1		-9.5		22.7	
$(^{R}PN^{H}P)_{3}Cu_{6}H_{6}$ $(^{R}PN^{H}P)_{2}Cu_{4}H_{4}$	1.0 10.8	2.07 (sept) 5.11 (quint)	-8.6 1.8	2.06 (sept) 5.04 (quint)	N/A 29.8	N/A 4.94 (quint)

a copper hydride in its mononuclear form, resulting in a copper alkoxide intermediate. Depending on the electrophilicity of the substrate, this step may or may not be faster than dissociation of the clusters into the monomer, as demonstrated by a recent study of $(NHC)_2Cu_2H_2$. However, DFT calculations of phosphine-ligated systems suggest that C=O insertion into a dinuclear copper hydride has a lower kinetic barrier than the mononuclear pathway. Experimental work on phosphine-based copper hydrides reacting with carbonyl compounds is surprisingly scarce in the literature. Stryker's reagent was shown to react with α,β -unsaturated ketones to form copper enolate complexes but found inert with cyclohexanone. The analogous cluster $[(p\text{-tolyl})_3P]_6Cu_6H_6$ was reported to react with HCHO to yield Tishchenko product HCO₂Me in a catalytic fashion.

Given these limited examples, we sought to investigate the reactions of our isolated copper hydride clusters with various carbonyl compounds. Treatment of 2a with PhCHO in C_6D_6 formed a major product tentatively assigned to a copper benzoxide complex³⁸ along with a small amount of 2a', PhCO₂CH₂Ph, and an unidentified product. The presence of 2a', though transient (observed only at the beginning of the reaction), provides direct evidence for the breakdown of the copper cluster during hydride transfer. The reaction of 2a with PhCOCH₃ was markedly slower, forming multiple products. The major species showed a quartet at 5.02 ppm and a doublet at 1.60 ppm, consistent with PhCOCH₃ being reduced to a copper-bound alkoxide complex.

We were particularly interested in knowing how the cluster size and phosphorus substituents would affect the abilities of copper hydrides to reduce carbonyl compounds. For comparison, N-methyl-2-pyrrolecarboxaldehyde was chosen as the substrate due to the following advantages: (1) This aldehyde undergoes a cleaner reduction. (2) Chemical shifts of the product are well-separated from those of the starting material. (3) Reduction reactions occur at rates convenient for NMR studies. In a typical experiment, a copper hydride cluster $(^{R}PN^{H}P)_{n}Cu_{2n}H_{2n}$ dissolved in $C_{6}D_{6}$ was mixed with N-methyl-2-pyrrolecarboxaldehyde in a 6:10 copper-to-aldehyde ratio, and the initial aldehyde concentration (0.082 M) was kept the same (eq 5).

$$(^{RPN^{H}P})_{n}Cu_{2n}H_{2n} + \bigvee_{Me} CHO \xrightarrow{C_{6}D_{6}} \bigvee_{Me} O [Cu]$$
 (5)

The hexanuclear cluster (^{iP}PN^HP)₃Cu₆H₆ (2a) was shown to reduce the aldehyde by 7% after 3 h and 27% after 6 h, at which point 2a had all but disappeared. This result implies an induction period for aldehyde reduction, which may be attributed to cluster dissociation, although we were unable to identify smaller copper hydride clusters or the mononuclear species. If all the copper-bound hydrogens behaved as hydride donors, then a maximum of 60% aldehyde conversion would be anticipated. The extent of aldehyde reduction at 6 h suggests that only ~50% of 2a acted as the reducing agent. Indeed, the ³¹P{¹H} NMR spectrum showed a broad resonance at 4.7 ppm (50%) for the insertion product³⁹ in addition to two resonances at 5.7 and 6.5 ppm (~25% for each), which were previously observed as decomposition products of 2a.

Pure $(^{Cy}PN^{H}P)_{2}Cu_{4}H_{4}$ (2b') was almost fully consumed in 1 h, converting 60% of the aldehyde to an alkoxide species. The insertion product featured a phosphorus resonance at

-4.1 ppm and a proton resonance at 4.98 ppm for the $ArCH_2O$ hydrogens. As mentioned earlier, it was not possible to obtain $(^{Cy}PN^HP)_3Cu_6H_6$ (2b) free of 2b'; therefore, the reduction was performed with a mixture of 2b (61 mol %) and 2b' (39 mol %). These two clusters disappeared within 3 h, in part to decomposition products, concurrently reducing 31% of the aldehyde. Comparing the reactivities of 2a and 2b was complicated by the nonproductive decomposition pathways and the purity of 2b; however, the tetranuclear cluster 2b' is clearly more reactive than both hexanuclear clusters.

Cluster (^{tBu}PN^HP)₂Cu₄H₄ (2c') showed virtually no reactivity toward *N*-methyl-2-pyrrolecarboxaldehyde. The reaction monitored for 24 h indicated that <1% of the aldehyde was converted. Furthermore, the solution color turned slightly yellow, in contrast to significant darkening of the solution observed for the reactions with 2a, 2b, and 2b'.

CONCLUSIONS

In this work, we have synthesized and characterized four different copper hydride clusters supported by the aminecentered diphosphine ligands HN(CH2CH2PR2)2. Unlike other metal hydrides stabilized by the same type of ligands, ^{14,40} the copper system does not involve nitrogen coordination. The steric properties of the phosphorus substituents play a critical role in controlling the size of the clusters. More specifically, isopropyl and cyclohexyl groups promote the growth of hexanuclear clusters (RPNHP)3Cu6H6, whereas tert-butyl groups favor the formation of a tetranuclear cluster (tBuPNHP)2Cu4H4. In the isopropyl and cyclohexyl cases, tetranuclear clusters can also be observed at the early stage of copper hydride formation but converted to the hexanuclear species. Structural elucidation using X-ray crystallography shows a distorted octahedral Cu₆ unit in (RPNHP)₃Cu₆H₆ and a tetrahedral Cu₄ unit in (RPNHP)₂Cu₄H₄. The hydride ligands are shown to cap the octahedral and tetrahedral faces, and found fluxional in solution. These copper hydride clusters, especially those bearing a less sterically hindered ligand, reduce aldehydes and ketones. The order of their reactivities toward N-methyl-2-pyrrolecarboxaldehyde is $(^{Cy}PN^{H}P)_{2}Cu_{4}H_{4} > (^{R}PN^{H}P)_{3}Cu_{6}H_{6}$ ($R = {}^{i}Pr$, Cy) $\gg (^{tBu}PN^{H}P)_{2}Cu_{4}H_{4}$, which correlates inversely with their thermal stabilities. Our future research in this area will be focused on studying the roles that these clusters play in catalytic processes including hydrogenation and hydrosilylation reactions.

EXPERIMENTAL SECTION

General Considerations. Unless otherwise mentioned, all copper complexes were prepared and handled under an inert atmosphere using standard Schlenk line and inert-atmosphere box techniques. Toluene, pentane, and THF were deoxygenated and dried in a solvent purification system by passing through an activated alumina column and an oxygen-scavenging column under argon. Acetonitrile was dried over calcium hydride and benzene-d₆ (99.5% D) was dried over sodium-benzophenone, after which both were distilled under an argon atmosphere. N-Methyl-2-pyrrolecarboxaldehyde was used as received from a commercial source (TCI Chemicals) without further purification. HN(CH₂CH₂PⁱPr₂)₂ (^{iP}rPN^HP), ^{22a,41} HN-(CH₂CH₂PCy₂)₂ (^{Cy}PN^HP), ⁴² HN(CH₂CH₂PⁱBu₂)₂ (^{iBu}PN^HP), ⁴³ and (^{iP}rPN^HP)CuBr (1a)¹⁷ were prepared according to literature procedures. Unless otherwise noted, NMR spectra were recorded at ambient temperature on a Bruker AV400 MHz or NEO400 MHz spectrometer. Chemical shift values for ¹H and ¹³C{¹H} NMR spectra were referenced internally to the residual solvent resonances. ³¹P{¹H} NMR spectra were referenced externally to 85% H₃PO₄ (0 ppm).

I

Infrared spectra were recorded on a PerkinElmer Spectrum Two FT-IR spectrometer equipped with a smart orbit diamond attenuated total reflectance (ATR) accessory.

Synthesis of (CypNHP)CuBr (1b). To an oven-dried Schlenk flask equipped with a stir bar were added CyPNHP (466 mg, 1.0 mmol), CuBr (144 mg, 1.0 mmol), and 50 mL of THF. The resulting mixture was stirred overnight and then filtered through a plug of Celite to yield a colorless solution, which was evaporated to dryness under vacuum. The residue was washed with pentane (7 mL \times 4) and dried under vacuum to afford the desired product as a white solid (493 mg, 81% yield). X-ray-quality, colorless crystals were grown at −30 °C from a saturated toluene solution layered with pentane. ¹H NMR (400 MHz, C_6D_6 , δ): 2.45–2.30 (m, NCH₂, 4H), 2.26 (br, NH, 1H), 1.93-1.85 (m, CyH, 8H), 1.81-1.69 (m, CyH, 12H), 1.67-1.62 (m, CyH, 4H), 1.56–1.42 (m, CyH, 8H), 1.37–1.31 (m, PCH₂, 4H), 1.29–1.18 (m, CyH, 12H). ${}^{13}C\{{}^{1}H\}$ NMR (101 MHz, C_6D_6 , δ): 45.6 (s, NCH₂), 34.6 (t, J_{P-C} = 6.7 Hz, PCH), 30.1 (s, CyC), 29.8 (s, CyC), 28.0 (t, J_{P-C} = 5.5 Hz, CyC), 27.7 (t, J_{P-C} = 5.5 Hz, CyC), 26.6 (s, CyC), 23.6 (t, J_{P-C} = 7.3 Hz, PCH₂). ³¹P{¹H} NMR (162 MHz, C_6D_6 , δ): -4.1 (s). Selected ATR-IR data (solid, cm⁻¹): 3221 (ν_{NH}), 2921, 2845, 1445, 1413, 1347, 1263, 1214, 1192, 1178, 1101, 1046, 1003. Anal. Calcd for C₂₈H₅₃BrCuNP₂: C, 55.21; H, 8.77; N, 2.30. Found: C, 55.36; H, 8.78; N, 2.31.

Synthesis of (^{t8ú}**PN**^H**P**)**CuBr** (**1c**). This compound was obtained as a white solid in 81% yield (1.5 mmol scale reaction) following a procedure similar to that used for **1b**. X-ray-quality, colorless crystals were grown from a saturated THF solution layered with pentane. ¹H NMR (400 MHz, C_6D_6 , δ): 2.62–2.49 (m, NCH₂, 4H), 1.39–1.32 (m, PCH₂, 4H), 1.28–1.21 (m, CH₃, 36H); the NH resonance was not located. ¹³C{¹H} NMR (101 MHz, C_6D_6 , δ): 44.4 (s, NCH₂), 33.6 (t, J_{P-C} = 5.8 Hz, $C(CH_3)_3$), 29.9 (t, J_{P-C} = 3.7 Hz, $C(CH_3)_3$), 19.2 (s, PCH₂). ³¹P{¹H} NMR (162 MHz, C_6D_6 , δ): 15.0 (s). Selected ATR-IR data (solid, cm⁻¹): 3271 (ν_{NH}), 2938, 2894, 2862, 2819, 2796, 1469, 1389, 1364, 1358, 1176, 1133. Anal. Calcd for $C_{20}H_{45}$ BrCuNP₂: C_6 , 47.57; H, 8.98; N, 2.77. Found: C_6 , 47.82; H, 9.22; N, 2.86.

Synthesis of (iPrPNHP)3Cu6H6 (2a). Method A from 1a. In a glovebox, an oven-dried pressure tube equipped with a stir bar was charged with 1a (220 mg, 0.49 mmol) and 5 mL of toluene. KO^tBu (55 mg, 0.49 mmol) was then added, followed by the addition of 2 mL of toluene to facilitate the mixing of KO^tBu with 1a. The tube was subsequently connected to a PTFE male-threaded adapter in a standard Fischer-Porter setup and taken out of the glovebox. The system was purged with H2 gas several times before being kept under 40 psig of H₂ pressure. The resulting mixture was stirred at room temperature for 1 h, during which time the solution color turned to bright orange. The remaining H2 gas was carefully vented, and the apparatus was brought back to the glovebox. The reaction mixture was filtered through a short plug of Celite or a Titan3 PTFE syringe filter. The filtrate was concentrated under vacuum until ~1 mL of the solvent was left. Acetonitrile was added, resulting in the formation of an orange precipitate. The solid was collected by filtration, washed with acetonitrile, and then dried under vacuum to yield a pure product (94 mg, 88% yield).

Method B from CuBr. In a glovebox, an oven-dried pressure tube equipped with a stir bar was charged with iPrPNHP (76 mg, 0.25 mmol), CuBr (72 mg, 0.50 mmol), and KO^tBu (56 mg, 0.50 mmol), followed by the addition of 5 mL of toluene to ensure mixing of the reagents. The rest of the procedure was similar to the one described above for Method A. The desired product was isolated in 55% yield (60 mg). X-ray-quality, orange-red crystals of 2a were grown from a toluene solution layered with acetonitrile and kept at -30 °C. ¹H NMR (400 MHz, C_6D_6 , δ): 3.57 (quint, $J_{H-H} = 8.0$ Hz, NH, 1H), 3.13-2.84 (m, NCH₂, 4H), 2.07 (sept, $J_{P-H} = 7.0$ Hz, CuH, 2H), 1.99–1.85 (m, $CH(CH_3)_2$, 2H), 1.85–1.70 (m, $CH(CH_3)_2 + PCH_2$, 4H), 1.69-1.60 (m, PCH₂, 2H), 1.50-1.37 (m, CH(CH₃)₂, 6H), 1.33-1.14 (m, $CH(CH_3)_2$, 18H); integrations were normalized to only one ^{iPr}PN^HP ligand. ¹³C{¹H} NMR (10 °C, 101 MHz, C_6D_6 , δ): 47.9 (br, NCH₂), 26.2-25.8 (m, PCH), 24.7 (br, PCH), 22.8 (s, PCH₂), 20.4 (br, CH₃), 19.8 (br, CH₃), 19.3 (br, CH₃), 17.8 (s, CH₃).

 31 P{ 1 H} NMR (162 MHz, C_6 D $_6$, δ): 1.0 (s). Selected ATR-IR data (solid, cm $^{-1}$): 3225 ($\nu_{\rm NH}$), 3190 ($\nu_{\rm NH}$), 2948, 2924, 2902, 2865, 1460, 1381, 1362, 1335, 1298, 1236, 1117, 1024.

Synthesis of $(^{Cy}PN^HP)_3Cu_6H_6$ (2b) and $(^{Cy}PN^HP)_2Cu_4H_4$ (2b'). Method A from 1b. In a glovebox, an oven-dried pressure tube equipped with a stir bar was charged with 1b (400 mg, 0.66 mmol) and 25 mL of toluene. KOtBu (74 mg, 0.66 mmol) was then added, followed by the addition of 5 mL of toluene to facilitate the mixing of KO^tBu with **1b**. The tube was subsequently connected to a PTFE male-threaded adapter in a standard Fischer-Porter setup and taken out of the glovebox. The system was purged with H2 gas several times before being kept under 40 psig of H₂ pressure. The resulting mixture was stirred at room temperature for 1 h, during which time the solution color turned to bright orange-red. The remaining H₂ gas was carefully vented, and the apparatus was brought back to the glovebox. The reaction mixture was quickly filtered through a short plug of Celite or a Titan3 PTFE syringe filter. The filtrate was concentrated under vacuum until ~1 mL of the solvent was left. Acetonitrile was added, resulting in the formation of a pink precipitate along with an orange-red oily material stuck on the flask wall. The suspension was filtered through another short plug of Celite or a new Titan3 PTFE syringe filter, and the filtrate was discarded. At this point, the orangered oily material remained in the flask but dissolved in cold (-30 °C) pentane and was passed through the same plug of Celite or syringe filter, which was repeatedly eluted with cold (-30 °C) pentane until the filtrate became very light colored. The combined pentane solutions were evaporated to dryness under vacuum to afford a red solid consisting mainly 2b (with 20-40 mol % being 2b', 173 mg, 88% combined yield). The off-white solid left on Celite or syringe filter was quickly eluted with toluene and the filtrate was dried under vacuum. The residual was washed with cold pentane to remove the colored impurity (2b) and then dried under vacuum to yield pure 2b' as a white powder (5.8 mg, 3.0% yield).

Method B from CuBr. In a glovebox, an oven-dried pressure tube equipped with a stir bar was charged with ^{Cy}PN^HP (233 mg, 0.50 mmol), CuBr (144 mg, 1.0 mmol), and KO'Bu (118 mg, 1.05 mmol), followed by the addition of 10 mL of toluene to mix all reagents together. The rest of the procedure was similar to the one described above for Method A, leading to the isolation of a white solid (pure 2b', 6.9 mg, 2.3% yield) and a red solid (a mixture of 2b and 2b', 250 mg, 84% yield).

X-ray-quality, dark red crystals of **2b** were obtained from an NMR sample of **2b**' (minor) and **2b** (major) in C_6D_6 left standing overnight. Detailed crystallographic data of **2b** are provided in the Supporting Information. Spectroscopic characterization data of **2b** are as follows. 1H NMR (400 MHz, C_6D_6 , δ): 3.60 (quint, J_{H-H} = 7.6 Hz, NH, 1H), 3.15–2.99 (m, NCH₂, 2H), 2.94–2.78 (m, NCH₂, 2H), 2.37–2.26 (m, CyH, 4H), 2.06 (sept, J_{P-H} = 7.2 Hz, CuH, 2H), 2.01–1.14 (m, CyH + PCH₂, 44H); integrations were normalized to only one $^{Cy}PN^HP$ ligand. $^{13}C\{^1H\}$ NMR (101 MHz, C_6D_6 , δ): 47.2 (NCH₂), 36.3 (PCH), 35.2 (PCH), 29.9, 29.6, 29.2, 28.5, 28.3, 27.8, 27.7, 27.2, 27.1, 26.8, 22.9 (PCH₂). $^{31}P\{^1H\}$ NMR (162 MHz, C_6D_6 , δ): – 8.6 (s). Selected ATR-IR data (solid, cm⁻¹): 3226 (ν_{NH}), 3173 (ν_{NH}), 2917, 2845, 1445, 1402, 1342, 1295, 1266, 1193, 1180, 1119, 1071, 1001; some of these bands may belong to **2b**'.

X-ray-quality, pale yellow-colorless dichroic crystals of 2b' were grown from a saturated toluene solution layered with acetonitrile and kept at -30 °C. The sample also yielded some red crystals (presumably due to the inevitable partial conversion of 2b' to 2b), although they were not suited for X-ray crystallographic study. Detailed crystallographic data of 2b' are provided in the Supporting Information. Spectroscopic characterization data of 2b' are as follows. ¹H NMR (400 MHz, C_6D_6 , δ): 5.04 (quint, $J_{P-H} = 14.4$ Hz, CuH, 2H), 3.47 (quint, $J_{H-H} = 8.0$ Hz, NH, 1H), 3.10–2.92 (m, NCH₂, 4H), 2.26–2.13 (m, CyH, 4H), 1.96–1.48 (m, CyH + PCH₂, 32H), 1.36–1.16 (m, CyH, 12H); integrations were normalized to only one ^{Cy}PN^HP ligand. ¹³C{¹H} NMR (101 MHz, C_6D_6 , δ): 48.8 (d, $J_{P-C} = 9.9$ Hz, NCH₂), 34.8 (d, $J_{P-C} = 15.8$ Hz, PCH), 29.4 (d, $J_{P-C} = 7.1$ Hz, CyC), 28.4 (d, $J_{P-C} = 2.9$ Hz, CyC), 27.8 (d, $J_{P-C} = 5.1$ Hz, CyC), 27.7 (d, $J_{P-C} = 2.5$ Hz, CyC), 27.0 (s, CyC), 22.6 (d, $J_{P-C} = 12.0$ Hz,

PCH₂). ${}^{31}P\{{}^{1}H\}$ NMR (162 MHz, C_6D_6 , δ): 1.8 (s). Selected ATR-IR data (solid, cm⁻¹): 2918, 2846, 1539, 1513, 1450, 1358, 1347, 1323, 1306, 1252, 1178, 1103, 1030, 999.

Synthesis of (^{tBu}PN^HP)₂Cu₄H₄ (2c'). Method A from 1c. This compound was isolated as an off-white solid in 41% yield (23 mg) from the reaction of 1c (116 mg, 0.23 mmol) with KO^tBu (34 mg, 0.30 mmol) under H₂. The procedure was similar to that used for 2a (Method A) except the H₂ pressure was raised to 80 psig, and the reaction time was extended to 4 h. During the course of the reaction, the solution color changed from colorless to mustard yellow.

Method B from CuBr. This compound was alternatively obtained in 57% yield (69 mg) from the reaction of CuBr (72 mg, 0.50 mmol) and $^{\rm fBu}{\rm PN}^{\rm HP}$ (90 mg, 0.25 mmol) with KO'Bu (56 mg, 0.50 mmol) under H₂. The procedure was similar to that used for **2a** (Method B) except the H₂ pressure was raised to 80 psig, and the reaction mixture was stirred for 40 min. X-ray-quality, light yellow crystals of **2c**' were grown from a toluene solution layered with acetonitrile and kept at $-30~^{\circ}{\rm C}$. $^{1}{\rm H}$ NMR (400 MHz, C₆D₆, δ): 4.94 (quint, $J_{\rm P-H}$ = 14.4 Hz, CuH, 2H), 3.54 (quint, $J_{\rm H-H}$ = 8.4 Hz, NH, 1H), 3.20–2.73 (m, NCH₂, 4H), 1.89–1.71 (m, PCH₂, 4H), 1.34 (d, $J_{\rm P-H}$ = 12.0 Hz, CH₃, 36H); integrations were normalized to only one $^{\rm fBu}{\rm PN}^{\rm HP}$ ligand. $^{13}{\rm C}^{\{1}{\rm H}\}$ NMR (101 MHz, C₆D₆, δ): 49.2 (d, $J_{\rm P-C}$ = 9.6 Hz, NCH₂), 33.1 (d, $J_{\rm P-C}$ = 8.1 Hz, PC(CH₃)₃), 30.0 (d, $J_{\rm P-C}$ = 8.5 Hz, CH₃), 22.0 (d, $J_{\rm P-C}$ = 8.6 Hz, PCH₂). $^{31}{\rm P}^{\{1}{\rm H}\}$ NMR (162 MHz, C₆D₆, δ): 29.8 (s). Selected ATR-IR data (solid, cm⁻¹): 3173 (ν_{NH}), 2938, 2893, 2864, 1470, 1453, 1387, 1363, 1335, 1181, 1107.

Synthesis of (^{Pr}PN^HP)₃Cu₆D₆ (2a-D), (^{Cy}PN^HP)_nCu_{2n}D_{2n} (2b-D and 2b'-D), and (^{IBu}PN^HP)₂Cu₄D₄ (2a'-D). These deuterated compounds were prepared from 1a–c and KO'Bu under D₂ (20 psig) using Method A described above. The presence of copper deuteride was confirmed by ²H NMR spectroscopy.

Conversion of 2b' to 2b. Under an argon atmosphere, freshly purified **2b'** (10 mg) was placed in a J. Young NMR tube and dissolved in ca. 0.3 mL of C_6D_6 . Under ambient temperature and light conditions, **2b'** was slowly converted to **2b**, accompanied by decomposition to the free ligand ($\delta_P = -9.5$ ppm), Cu(0) (a black precipitate), and H_2 ($\delta_H = 4.47$ ppm). This process was monitored by 1H and $^{31}P\{^1H\}$ NMR spectroscopy for >40 days.

In Situ Generation of 2a' and 2a. To a dry Wilmad Quick Pressure Valve NMR tube were added 1a (6.7 mg, 15 μ mol), KO'Bu (2.0 mg, 18 μ mol), and ca. 0.25 mL of C_6D_6 . The mixture was degassed via a freeze–pump–thaw cycle and then placed under H_2 pressure (50 psig). NMR spectra were recorded after 30 min of mixing, at which point the solution color was orange. Selected ¹H NMR data (400 MHz, C_6D_6 , δ): 5.11 (quint, J_{P-H} = 14.2 Hz, CuH of 2a'), 2.11–2.01 (m, CuH of 2a). ³¹P{¹H} NMR (162 MHz, C_6D_6 , δ): 10.8 (br, 2a'), 1.0 (br, 2a), -1.1 (br, ^{1P}rPN^HP).

Reactions of the Copper Hydrides (2a, 2b, 2b', and 2c') with N-Methyl-2-pyrrolecarboxaldehyde. To a dry J. Young NMR tube were added a copper hydride (20 μ mol Cu), N-methyl-2-pyrrolecarboxaldehyde (3.6 μ L, 33 μ mol), and 400 μ L of C₆D₆. The tube was secured to a rotation device (e.g., a rotavap) that allowed constant mixing of the reaction. The progress of the reaction (at 23 °C) was periodically monitored by NMR spectroscopy. As the reaction proceeded, the solution slowly turned dark.

X-ray Structure Determinations. The conditions under which single crystals were grown are described in preceding sections for compound synthesis. Intensity data for **1b** were collected at 150 K on a Bruker PHOTON100 CMOS detector at Beamline 11.3.1 at the Advanced Light Source (Lawrence Berkeley National Laboratory) using synchrotron radiation tuned to $\lambda = 0.7749$ Å. Intensity data for **1c** and **2c**' were collected at 150 K on a Bruker APEX-II CCD diffractometer using graphite-monochromated Mo K α radiation ($\lambda = 0.71073$ Å). Intensity data for **2a**, **2b**, and **2b**' were collected at 150 K on a Bruker D8 Venture Mo–I μ S Photon-II diffractometer ($\lambda = 0.71073$ Å). The data frames were collected and processed using the program SAINT. The data were corrected for decay, Lorentz, and polarization effects as well as absorption and beam corrections. The structures were solved by a combination of direct methods and the difference Fourier technique and refined by full-matrix least-squares

on F^2 using the SHELX suite of programs. Non-hydrogen atoms were refined with anisotropic displacement parameters. The NH and CuH hydrogen atoms were located directly from the difference map, and the position was refined, with the exception of the disordered NH hydrogen atoms in **2b** (the positions of which were not refined). All remaining hydrogen atoms were calculated and treated with a riding model. Compound **2a** crystallizes with toluene in the lattice; the toluene molecule is disordered over the inversion center and refined at half-occupancy. For structure **2b**, N2 and C6 atoms are disordered and required distance restraints (refined major occupancy = 78%). The crystal structures for **1b**, **1c**, **2a**, **2b**, **2b'**, and **2c'** have been deposited at the Cambridge Crystallographic Data Centre (CCDC) and allocated the deposition numbers CCDC 2011131–2011136.

ASSOCIATED CONTENT

Supporting Information

The Supporting Information is available free of charge at https://pubs.acs.org/doi/10.1021/acs.inorgchem.0c01865.

Characterization data (NMR, IR, and X-ray diffraction) for the copper complexes and additional experimental details (PDF)

Accession Codes

CCDC 2011131–2011136 contain the supplementary crystallographic data for this paper. These data can be obtained free of charge via www.ccdc.cam.ac.uk/data_request/cif, or by emailing data_request@ccdc.cam.ac.uk, or by contacting The Cambridge Crystallographic Data Centre, 12 Union Road, Cambridge CB2 1EZ, UK; fax: +44 1223 336033.

AUTHOR INFORMATION

Corresponding Author

Hairong Guan — Department of Chemistry, University of Cincinnati, Cincinnati, Ohio 45221-0172, United States; orcid.org/0000-0002-4858-3159; Email: hairong.guan@uc.edu

Authors

Dewmi A. Ekanayake — Department of Chemistry, University of Cincinnati, Cincinnati, Ohio 45221-0172, United States

Arundhoti Chakraborty — Department of Chemistry, University of Cincinnati, Cincinnati, Ohio 45221-0172, United States

Jeanette A. Krause — Department of Chemistry, University of Cincinnati, Cincinnati, Ohio 45221-0172, United States

Complete contact information is available at: https://pubs.acs.org/10.1021/acs.inorgchem.0c01865

Notes

The authors declare no competing financial interest.

ACKNOWLEDGMENTS

We thank the NSF Chemical Catalysis Program for support of this research project (CHE-1800151) and the NSF MRI Program for support of the instrumentation used in this study, which include a Bruker APEX-II CCD diffractometer (CHE-0215950), a Bruker D8 Venture diffractometer (CHE-1625737), and a Bruker NEO400 MHz NMR spectrometer (CHE-1726092). Some of the crystallographic data described in this paper were collected through the SCrALS (Service Crystallography at Advanced Light Source) Program at Beamline 11.3.1 at the Advanced Light Source (ALS), Lawrence Berkeley National Laboratory. The ALS is supported by the U.S. Department of Energy, Office of Energy Sciences

Materials Sciences Division, under contract DE-AC02-05CH11231.

REFERENCES

- (1) (a) Deutsch, C.; Krause, N.; Lipshutz, B. H. CuH-Catalyzed Reactions. *Chem. Rev.* **2008**, *108*, 2916–2927. (b) Jordan, A. J.; Lalic, G.; Sadighi, J. P. Coinage Metal Hydrides: Synthesis, Characterization, and Reactivity. *Chem. Rev.* **2016**, *116*, 8318–8372.
- (2) (a) Romero, E. A.; Olsen, P. M.; Jazzar, R.; Soleilhavoup, M.; Gembicky, M.; Bertrand, G. Spectroscopic Evidence for a Monomeric Copper(I) Hydride and Crystallographic Characterization of a Monomeric Silver(I) Hydride. *Angew. Chem., Int. Ed.* **2017**, *56*, 4024–4027. (b) Xu, G.; Leloux, S.; Zhang, P.; Meijide Suárez, J.; Zhang, Y.; Derat, E.; Ménand, M.; Bistri-Aslanoff, O.; Roland, S.; Leyssens, T.; Riant, O.; Sollogoub, M. Capturing the Monomeric (L)CuH in NHC-Capped Cyclodextrin: Cavity-Controlled Chemoselective Hydrosilylation of α,β -Unsaturated Ketones. *Angew. Chem., Int. Ed.* **2020**, *59*, 7591–7597.
- (3) (a) Bezman, S. A.; Churchill, M. R.; Osborn, J. A.; Wormald, J. Preparation and Crystallographic Characterization of a Hexameric Triphenylphosphinecopper Hydride Cluster. *J. Am. Chem. Soc.* 1971, 93, 2063–2065. (b) Churchill, M. R.; Bezman, S. A.; Osborn, J. A.; Wormald, J. Synthesis and Molecular Geometry of Hexameric Triphenylphosphinocopper(I) Hydride and the Crystal Structure of H₆Cu₆(PPh₃)₆·HCONMe₂. *Inorg. Chem.* 1972, 11, 1818–1825. (4) (a) Baker, B. A.; Bošković, Z. V.; Lipshutz, B. H. (BDP)CuH: A
- (4) (a) Baker, B. A.; Bošković, Ž. V.; Lipshutz, B. H. (BDP)CuH: A "Hot" Stryker's Reagent for Use in Achiral Conjugate Reductions. *Org. Lett.* **2008**, *10*, 289–292. (b) Motokura, K.; Kashiwame, D.; Miyaji, A.; Baba, T. Copper-Catalyzed Formic Acid Synthesis from CO₂ with Hydrosilanes and H₂O. *Org. Lett.* **2012**, *14*, 2642–2645.
- (5) Eberhart, M. S.; Norton, J. R.; Zuzek, A.; Sattler, W.; Ruccolo, S. Electron Transfer from Hexameric Copper Hydrides. *J. Am. Chem. Soc.* **2013**, *135*, 17262–17265.
- (6) Goeden, G. V.; Huffman, J. C.; Caulton, K. G. A Cu–(μ -H) Bond Can Be Stronger Than an Intramolecular P \rightarrow Cu Bond. Synthesis and Structure of Cu₂(μ -H)₂[η ²-CH₃C(CH₂PPh₂)₃]₂. *Inorg. Chem.* **1986**, *25*, 2484–2485.
- (7) Xi, Y.; Hartwig, J. F. Mechanistic Studies of Copper-Catalyzed Asymmetric Hydroboration of Alkenes. *J. Am. Chem. Soc.* **2017**, *139*, 12758–12772.
- (8) Albert, C. F.; Healy, P. C.; Kildea, J. D.; Raston, C. L.; Skelton, B. W.; White, A. H. Lewis-Base Adducts of Group 11 Metal(I) Compounds. 49. Structural Characterization of Hexameric and Pentameric (Triphenylphosphine)copper(I) Hydrides. *Inorg. Chem.* 1989, 28, 1300–1306.
- (9) (a) Ho, D. M.; Bau, R. The Skeletal Bonding and Structure of $H_6Cu_6(PR_3)_6$ Clusters. X-Ray and Topological Studies on the $H_6Cu_6[P(p\text{-tolyl})_3]_6$ Molecule. *Inorg. Chim. Acta* **1984**, *84*, 213–220. (b) Stevens, R. C.; McLean, M. R.; Bau, R.; Koetzle, T. F. Neutron Diffraction Structure Analysis of a Hexanuclear Copper Hydrido Complex, $H_6Cu_6[P(p\text{-tolyl})_3]_6$: An Unexpected Finding. *J. Am. Chem. Soc.* **1989**, *111*, 3472–3473. (c) Lemmen, T. H.; Folting, K.; Huffman, J. C.; Caulton, K. G. Copper Polyhydrides. *J. Am. Chem. Soc.* **1985**, *107*, 7774–7775.
- (10) (a) Dhayal, R. S.; van Zyl, W. E.; Liu, C. W. Polyhydrido Copper Clusters: Synthetic Advances, Structural Diversity, and Nanocluster-to-Nanoparticle Conversion. *Acc. Chem. Res.* **2016**, *49*, 86–95. (b) Liu, X.; Astruc, D. Atomically Precise Copper Nanoclusters and Their Applications. *Coord. Chem. Rev.* **2018**, *359*, 112–126. (c) Dhayal, R. S.; van Zyl, W. E.; Liu, C. W. Copper Hydride Clusters in Energy Storage and Conversion. *Dalton Trans.* **2019**, *48*, 3531–3538.
- (11) Brocha Silalahi, R. P.; Huang, G.-R.; Liao, J.-H.; Chiu, T.-H.; Chakrahari, K. K.; Wang, X.; Cartron, J.; Kahlal, S.; Saillard, J.-Y.; Liu, C. W. Copper Clusters Containing Hydrides in Trigonal Pyramidal Geometry. *Inorg. Chem.* **2020**, *59*, 2536–2547.
- (12) Nguyen, T.-A. D.; Goldsmith, B. R.; Zaman, H. T.; Wu, G.; Peters, B.; Hayton, T. W. Synthesis and Characterization of a Cu₁₄

- Hydride Cluster Supported by Neutral Donor Ligands. *Chem. Eur. J.* **2015**, 21, 5341–5344.
- (13) (a) Chakraborty, S.; Dai, H.; Bhattacharya, P.; Fairweather, N. T.; Gibson, M. S.; Krause, J. A.; Guan, H. Iron-Based Catalysts for the Hydrogenation of Esters to Alcohols. J. Am. Chem. Soc. 2014, 136, 7869-7872. (b) Fairweather, N. T.; Gibson, M. S.; Guan, H. Homogeneous Hydrogenation of Fatty Acid Methyl Esters and Natural Oils under Neat Conditions. Organometallics 2015, 34, 335-339. (c) Dai, H.; Guan, H. Switching the Selectivity of Cobalt-Catalyzed Hydrogenation of Nitriles. ACS Catal. 2018, 8, 9125-9130. (14) (a) Schneider, S.; Meiners, J.; Askevold, B. Cooperative Aliphatic PNP Amido Pincer Ligands - Versatile Building Blocks for Coordination Chemistry and Catalysis. Eur. J. Inorg. Chem. 2012, 2012, 412-429. (b) Werkmeister, S.; Junge, K.; Wendt, B.; Alberico, E.; Jiao, H.; Baumann, W.; Junge, H.; Gallou, F.; Beller, M. Hydrogenation of Esters to Alcohols with a Well-Defined Iron Complex. Angew. Chem., Int. Ed. 2014, 53, 8722-8726. (c) Chakraborty, S.; Lagaditis, P. O.; Förster, M.; Bielinski, E. A.; Hazari, N.; Holthausen, M. C.; Jones, W. D.; Schneider, S. Well-Defined Iron Catalysts for the Acceptorless Reversible Dehydrogenation-Hydrogenation of Alcohols and Ketones. ACS Catal. 2014, 4, 3994-4003.
- (15) Liu, S.; Eberhart, M. S.; Norton, J. R.; Yin, X.; Neary, M. C.; Paley, D. W. Cationic Copper Hydride Clusters from Oxidation of (Ph₃P)₆Cu₆H₆. *J. Am. Chem. Soc.* **2017**, *139*, 7685–7688.
- (16) Brestensky, D. M.; Huseland, D. E.; McGettigan, C.; Stryker, J. M. Simplified, "One-Pot" Procedure for the Synthesis of [(Ph₃P)-CuH]₆, a Stable Copper Hydride for Conjugate Reductions. *Tetrahedron Lett.* **1988**, 29, 3749–3752.
- (17) Rozenel, S. S.; Kerr, J. B.; Arnold, J. Metal Complexes of Co, Ni and Cu with the Pincer Ligand HN(CH₂CH₂PⁱPr₂)₂: Preparation, Characterization and Electrochemistry. *Dalton Trans.* **2011**, *40*, 10397–10405.
- (18) $\tau_4 = (360 \alpha \beta)/141$; α and β are the two largest bond angles (in degrees). For details, see Yang, L.; Powell, D. R.; Houser, R. P. Structural Variation in Copper(I) Complexes with Pyridylmethylamide Ligands: Structural Analysis with a New Four-Coordinate Geometry Index, τ_4 . Dalton Trans. 2007, 955–964.
- (19) Garrou, P. E. Δ_R Ring Contributions to ³¹P NMR Parameters of Transition-Metal-Phosphorus Chelate Complexes. *Chem. Rev.* **1981**, *81*, 229–266.
- (20) Petöcz, G.; Berente, Z.; Kégl, T.; Kollár, L. Xantphos as cis- and trans-Chelating Ligand in Square-Planar Platinum(II) Complexes. Hydroformylation of Styrene with Platinum—xantphos—tin(II)-chloride System. *J. Organomet. Chem.* **2004**, *689*, 1188—1193.
- (21) Kaltzoglou, A.; Fässler, T. F.; Aslanidis, P. A Luminescent Copper(I) Bromide Complex Chelated with 4,5-Bis-(diphenylphosphano)-9,9-dimethyl-xanthene. *J. Coord. Chem.* **2008**, 61, 1774–1781.
- (22) (a) Clarke, Z. E.; Maragh, P. T.; Dasgupta, T. P.; Gusev, D. G.; Lough, A. J.; Abdur-Rashid, K. A Family of Active Iridium Catalysts for Transfer Hydrogenation of Ketones. *Organometallics* **2006**, *25*, 4113–4117. (b) Fillman, K. L.; Bielinski, E. A.; Schmeier, T. J.; Nesvet, J. C.; Woodruff, T. M.; Pan, C. J.; Takase, M. K.; Hazari, N.; Neidig, M. L. Flexible Binding of PNP Pincer Ligands to Monomeric Iron Complexes. *Inorg. Chem.* **2014**, *53*, 6066–6072. (c) Wellala, N. P. N.; Luebking, J. D.; Krause, J. A.; Guan, H. Roles of Hydrogen Bonding in Proton Transfer to κ^P,κ^N,κ^P-N(CH₂CH₂PⁱPr₂)₂-Ligated Nickel Pincer Complexes. *ACS Omega* **2018**, *3*, 4986–5001.
- (23) This hydride resonance falls slightly outside the range of the reported values for phosphine-based, neutral copper hydride complexes (4.18–0.60 ppm).
- (24) Bondi, A. van der Waals Volumes and Radii. J. Phys. Chem. 1964, 68, 441-451.
- (25) Bennett, E. L.; Murphy, P. J.; Imberti, S.; Parker, S. F. Characterization of the Hydrides in Stryker's Reagent: $[HCu\{P-(C_6H_5)_3\}]_6$. Inorg. Chem. **2014**, 53, 2963–2967.
- (26) In a recent study, interstitial hydrides in Cu-Ag clusters were anisotropically refined to convergence using X-ray diffraction data. For details, see Zhong, Y.-J.; Liao, J.-H.; Chiu, T.-H.; Wu, Y.-Y.;

- Kahlal, S.; Saillard, J.-Y.; Liu, C. W. Hydride-Encapsulated Bimetallic Clusters Supported by 1,1-Dithiolates. *Chem. Commun.* **2020**, *56*, 9300–9303.
- (27) Nie, H.-H.; Han, Y.-Z.; Tang, Z.; Yang, S.-Y.; Teo, B. K. Hydride Induced Formation and Optical Properties of Tetrahedral $[Cu_4(\mu_4-H)(\mu_2-X)_2(PPh_2Py)_4]^+$ Clusters (X = Cl, Br; Py = pyridyl). *J. Cluster Sci.* **2018**, 29, 837–846.
- (28) Nakajima, T.; Nakamae, K.; Hatano, R.; Imai, K.; Harada, M.; Ura, Y.; Tanase, T. Tetra-, Hexa- and Octanuclear Copper Hydride Complexes Supported by Tridentate Phosphine Ligands. *Dalton Trans.* **2019**, *48*, 12050–12059.
- (29) Nakamae, K.; Kure, B.; Nakajima, T.; Ura, Y.; Tanase, T. Facile Insertion of Carbon Dioxide into $Cu_2(\mu-H)$ Dinuclear Units Supported by Tetraphosphine Ligands. *Chem. Asian J.* **2014**, *9*, 3106–3110.
- (30) Nakajima, T.; Kamiryo, Y.; Hachiken, K.; Nakamae, K.; Ura, Y.; Tanase, T. Tri- and Tetranuclear Copper Hydride Complexes Supported by Tetradentate Phosphine Ligands. *Inorg. Chem.* **2018**, *57*, 11005–11018.
- (31) Kounalis, E.; Lutz, M.; Broere, D. L. J. Cooperative H₂ Activation on Dicopper(I) Facilitated by Reversible Dearomatization of an "Expanded PNNP Pincer" Ligand. *Chem. Eur. J.* **2019**, 25, 13280–13284.
- (32) (a) Custelcean, R.; Jackson, J. E. Dihydrogen Bonding: Structures, Energetics, and Dynamics. *Chem. Rev.* **2001**, *101*, 1963–1980. (b) Belkova, N. V.; Epstein, L. M.; Filippov, O. A.; Shubina, E. S. Hydrogen and Dihydrogen Bonds in the Reactions of Metal Hydrides. *Chem. Rev.* **2016**, *116*, 8545–8587.
- (33) Goeden, G. V.; Caulton, K. G. Soluble Copper Hydrides: Solution Behavior and Reactions Related to CO Hydrogenation. J. Am. Chem. Soc. 1981, 103, 7354–7355.
- (34) (a) Mankad, N. P.; Laitar, D. S.; Sadighi, J. P. Synthesis, Structure, and Alkyne Reactivity of a Dimeric (Carbene)copper(I) Hydride. *Organometallics* **2004**, *23*, 3369–3371. (b) Frey, G. D.; Donnadieu, B.; Soleilhavoup, M.; Bertrand, G. Synthesis of a Room-Temperature-Stable Dimeric Copper (I) Hydride. *Chem. Asian J.* **2011**, *6*, 402–405. (c) Jordan, A. J.; Wyss, C. M.; Bacsa, J.; Sadighi, J. P. Synthesis and Reactivity of New Copper(I) Hydride Dimers. *Organometallics* **2016**, *35*, 613–616.
- (35) Tran, B. L.; Neisen, B. D.; Speelman, A. L.; Gunasekara, T.; Wiedner, E. S.; Bullock, R. M. Mechanistic Studies on the Insertion of Carbonyl Substrates into Cu-H: Different Rate-Limiting Steps as a Functional of Electrophilicity. *Angew. Chem., Int. Ed.* **2020**, *59*, 8645–8653.
- (36) Zatolochnaya, O. V.; Rodríguez, S.; Zhang, Y.; Lao, K. S.; Tcyrulnikov, S.; Li, G.; Wang, X.-J.; Qu, B.; Biswas, S.; Mangunuru, H. P. R.; Rivalti, D.; Sieber, J. D.; Desrosiers, J.-N.; Leung, J. C.; Grinberg, N.; Lee, H.; Haddad, N.; Yee, N. K.; Song, J. J.; Kozlowski, M. C.; Senanayake, C. H. Copper-Catalyzed Asymmetric Hydrogenation of 2-Substituted Ketones via Dynamic Kinetic Resolution. *Chem. Sci.* **2018**, *9*, 4505–4510.
- (37) Mahoney, W. S.; Stryker, J. M. Hydride-Mediated Homogeneous Catalysis. Catalytic Reduction of α,β -Unsaturated Ketones Using [(Ph₃P)CuH]₆ and H₂. *J. Am. Chem. Soc.* **1989**, *111*, 8818–8823.
- (38) A singlet in the 5.32–4.74 ppm region was observed, which shifted during the course of the reaction, possibly due to exchange of a copper-bound benzoxide with adventitious water. This phenomenon was previously noticed in the insertion reaction of PhCHO with a nickel hydride complex. For details, see Chakraborty, S.; Krause, J. A.; Guan, H. Hydrosilylation of Aldehydes and Ketones Catalyzed by Nickel PCP-Pincer Hydride Complexes. *Organometallics* **2009**, 28, 582–586.
- (39) The nuclearity of the insertion product and the coordination mode for the ^{iPr}PN^HP ligand are unknown. Unfortunately, it was not possible to isolate the insertion product because of its high sensitivity.

 (40) Vasudevan K V Scott B L Hanson S K Alkene
- (40) Vasudevan, K. V.; Scott, B. L.; Hanson, S. K. Alkene Hydrogenation Catalyzed by Nickel Hydride Complexes of an

- Aliphatic PNP Pincer Ligand. Eur. J. Inorg. Chem. 2012, 2012, 4898-4906.
- (41) Bertoli, M.; Choualeb, A.; Gusev, D. G.; Lough, A. J.; Major, Q.; Moore, B. PNP Pincer Osmium Polyhydrides for Catalytic Dehydrogenation of Primary Alcohols. *Dalton Trans.* **2011**, *40*, 8941–8949.
- (42) Ma, W.; Cui, S.; Sun, H.; Tang, W.; Xue, D.; Li, C.; Fan, J.; Xiao, J.; Wang, C. Iron-Catalyzed Alkylation of Nitriles with Alcohols. *Chem. Eur. J.* **2018**, *24*, 13118–13123.
- (43) (a) Abdur-Rashid, K.; Graham, T.; Tsang, C.-W.; Chen, X.; Guo, R.; Jia, W.; Amoroso, D.; Sui-Seng, C. Method for the Production of Hydrogen from Ammonia Borane. WO 2008/141439. (b) Meiners, J.; Friedrich, A.; Herdtweck, E.; Schneider, S. Facile Double C–H Activation of Tetrahydrofuran by an Iridium PNP Pincer Complex. *Organometallics* 2009, 28, 6331–6338.